Structural Fluctuations, Spin, Reorganization Energy, and Tunneling Energy Control of Intramolecular Electron Transfer: The Surprising Case of Electron Transfer in a d8−d8 Bimetall...

ARTICLE *in* JOURNAL OF THE AMERICAN CHEMICAL SOCIETY · JUNE 1997

Impact Factor: 12.11 · DOI: 10.1021/ja970309r

Structural Fluctuations, Spin, Reorganization Energy, and Tunneling Energy Control of Intramolecular Electron Transfer: The Surprising Case of Electron Transfer in a d^8-d^8 Bimetallic System

I. V. Kurnikov,[†] L. D. Zusman,[†,‡] M. G. Kurnikova,[†] R. S. Farid,[§] and D. N. Beratan*,[†]

Contribution from the Department of Chemistry, University of Pittsburgh, Pittsburgh, Pennsylvania 15260, Institute of Inorganic Chemistry, Novosibirsk, Russia 630090, and Department of Chemistry, Rutgers University, 73 Warren Street, Newark, New Jersey 07102

Received January 29, 1997[⊗]

Abstract: A considerable body of unimolecular electron-transfer rate data has been reported recently for Ir_2 excited-state donors linked to substituted pyridinium acceptors. These data pose a substantial paradox. Simple analysis suggested that donor−acceptor coupling matrix elements differ by 1 order of magnitude for the excited triplet and singlet states. Yet, there is no fundamental reason to expect this large electronic coupling dependence on spin state. We offer an alternative self-consistent interpretation based on a hybrid theoretical analysis that includes *ab initio* quantum calculations of electronic couplings, molecular dynamics simulations of molecular geometries, and Poisson−Boltzmann computations of reorganization energies. Taken together the analysis provides a detailed comprehensive interpretation of these reactions. In our analysis, we reach the conclusions: (1) that reorganization energies in these systems (∼1.3−1.7 eV) are larger than expected from simple analysis of experiments, (2) that electronic couplings (∼0.005−0.02 eV) are also larger than previously believed and differ only by a factor of 2 for singlet and triplet states, (3) that the molecules have access to multiple conformations differing both in reorganization energy and electronic coupling, and explicit treatment of this flexibility is crucial to interpret the rate data, and (4) that a considerable dip is expected in the donor−acceptor coupling dependence on tunneling energy, associated with destructively interfering electron and hole-mediated coupling pathways, which probably leads to a small observed ET rate in one of the compounds. Taken together, this analysis explains most of the experimental data. Fundamental arguments and detailed computations show that the influence of donor spin state on long-range electronic interactions is relatively weak. Many of the molecular aspects that establish the ET characteristics of these molecules exist in other semirigid model compounds, making this hybrid theoretical strategy of general interest.

I. Introduction

A general framework exists to interpret electron-transfer (ET) reactions and their dependence upon molecular structure.[1,2] The major physical factors that control ET reaction rates, including reaction free energy change, outer-sphere and inner-sphere reorganization energies, and electronic coupling, have been identified. Yet, many challenges remain in the quantitative determination of these factors because, in most situations, it is not easy to relate them directly to experimental quantities. Theoretical studies of ET reactions using modern molecular modeling techniques should provide a better understanding of the reaction mechanisms, leading to detailed quantitative descriptions of the molecular systems. Much progress toward molecular-level descriptions has been reported for studies of both small and large systems in recent years.[3,4] This paper attempts to reconcile a family of ET rate data, some of which are extremely provocative. Our goals are to construct a detailed and predictive theoretical description of these reactions using a battery of molecular modeling techniques. We hope that treatments of this kind will lead to the development a set of reliable theoretical tools to study a broad range of charge-transfer reactions in solution.

The experiments described in refs 5−8 examined photoinduced ET in compounds with pyrazolate-bridged iridium(I) dimers (Ir_2) as photoreductants covalently bound through phosphonite ligands to alkyl pyridinium acceptors. The molecular linker connecting Ir_2 and pyridinium was varied, as was the substituent attached to the pyridinium ring. These structural features control the bridge-mediated electronic coupling and the thermodynamic driving force of the ET reaction, respectively. The structures of these compounds are shown in Figure 1. As we will see, the nature of the linker also controls the conformational dynamics of the molecule.

Reactions studied experimentally included photoinduced ET from the singlet and triplet excited states of Ir_2 to the pyridinium acceptor, as well as charge recombination. Experimental ET rates were obtained from fluorescence quantum yield and transient-absorption measurements. Free energy changes were estimated from the measured redox potentials of donor and acceptor groups, and the vertical excitation energies of the

[†] University of Pittsburgh.
[‡] Institute of Inorganic Chemistry.
[§] Rutgers University.
[⊗] Abstract published in *Advance ACS Abstracts,* June 1, 1997.

(1) Marcus, R. A.; Sutin, N. *Biochim. Biophys. Acta* **1985**, *811*, 265−322.
(2) Bendall, D. S., Ed. *Protein Electron Transfer*: BIOS Scientific Publishers Ltd.: Oxford, UK, 1996.
(3) Newton, M. D. *Chem. Rev.* **1991**, *91*, 767−792.
(4) Jordan, K. D.; Paddon-Row, M. N. *Chem. Rev.* **1992**, *92*, 395−410.
(5) Fox, L. S.; Kozik, M.; Winkler, J. R.; Gray, H. B. *Science* **1990**, *247*, 1069−1071.
(6) Farid, R. S.; Fox, L. S.; Gray, H. B.; Kozik, M.; Chang, I. J.; Winkler, J. *Mol. Cryst. Liq. Cryst.* **1991**, *194*, 259−262.
(7) Farid, R. S.; Chang, I. J.; Winkler, J. R.; Gray, H. B. *J. Phys. Chem.* **1994**, *98*, 5176−5179.
(8) Farid, S. Ph.D. Dissertation, California Institute of Technology, Pasadena, CA, 1991.

S0002-7863(97)00309-0 CCC: $14.00

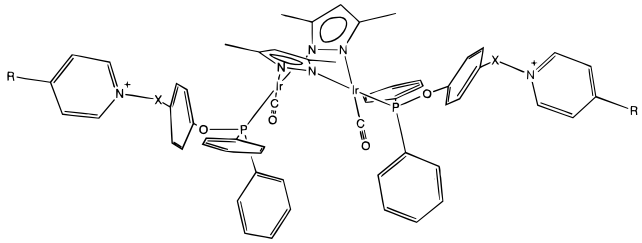

X = –	R = H	PC0
X = CH_2	R = H	PC1
X = CH_2	R = t-Bu	PC1-tBu
X = CH_2	R = Am	PC1-Am
X = $(CH_2)_2$	R = H	PC2
X = $(CH_2)_3$	R = H	PC3

Figure 1. Structures of the donor−acceptor complexes.

donor.[8] In this theoretical study, we examined the forward ET processes, as the rate constants of charge recombination (deduced from biexponential kinetics associated with ground-state recovery) are likely to be less reliable. Actually, from the results of this study, we expect that forward ET will have nonexponential kinetics because multiple molecular configurations are involved.

The standard high-temperature nonadiabatic ET rate expression, appropriate for ET reactions in weakly interacting donor−acceptor systems is[1]

$$k_{ET} = \frac{2\pi}{\hbar}\frac{1}{\sqrt{4\pi\lambda kT}}|H_{DA}|^2 \exp\left[-\frac{(\Delta G^\circ + \lambda)^2}{4\lambda kT}\right] \quad (1.1)$$

Three key factors control the nonadiabatic ET rate in equation 1.1: H_{DA}, the donor−acceptor electronic coupling that may be provided by direct donor−acceptor interaction or mediated by a molecular bridge or solvent; ΔG°, the reaction free energy change; and λ, the reorganization energy associated with changes in the equilibrium nuclear geometries of the redox centers (inner sphere) and changes in the equilibrium solvation accompanying ET (outer sphere). Here k is Boltzmann's constant, $\hbar$ is Planck's constant divided by 2π, and T is the temperature. Equation 1.1 predicts that the log of the ET rate will be a quadratic function of reaction free energy, ΔG°, with a maximum at $\Delta G^\circ = -\lambda$. This dependence, predicted more than 30 years ago,[9] eluded direct observation until the 1980s.[10−16]

The log(rate) data for the Ir_2-bridge−pyridinium species[6−8] show a nonmonotonic dependence of singlet excited-state electron transfer quenching rates on reaction free energy in the series of compounds PC1-tBu, PC1, and PC1-Am (see structures in Figure 1 and rate data in Table 1 and Figure 2). Assuming that the electronic coupling and reorganization energies are the same in these three compounds, a fit to equation 1.1 yields $H_{DA} = 6 \times 10^{-4}$ eV and $\lambda = 1.05$ eV for singlet excited state ET (see Figure 2).

Table 1. Experimental ET Rates in Ir_2−(Bridge)−Pyr^+

compound	singlet $-\Delta G^\circ$ (eV)	^{1}ET k_{ET} (s^{-1})	triplet $-\Delta G^\circ$ (eV)	^{3}ET k_{ET} (s^{-1})
PC0	0.90	1.0×10^{11} [a]	0.40	8.9×10^5 [a]
PC1-tBu	0.53	1.3×10^9 [a]	0.03	1.8×10^5 [a]
PC1	0.76	3.6[a] $(4.9$[b]$) \times 10^9$	0.26	2.5×10^5 [a]
PC1-Am	1.16	1.8[a] $(2.8$[b]$) \times 10^9$	0.66	2.4×10^5 [a]
PC2	0.67	1.4[a] $(0.99$[b]$) \times 10^{10}$	0.17	1.6×10^8 [a]
PC3	0.69	2.7×10^9 [a]	0.19	2.1×10^7 [a]

[a] From ref 8. [b] From ref 7.

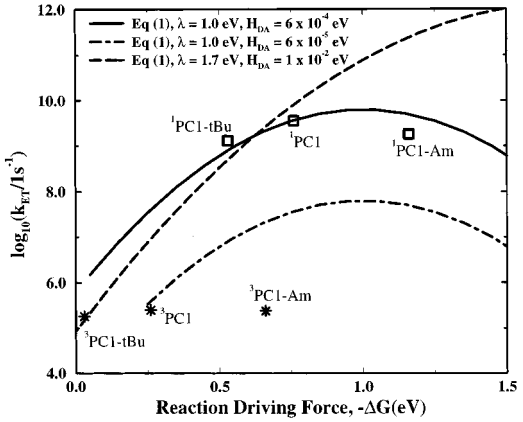

Figure 2. Experimental dependence of ET rates on reaction driving force in the PC1-*x* species. The original interpretation is based on a reorganization energy of ∼1.0 eV and a smaller value of H_{DA} for the triplet state ET (dash−dotted line) compared to singlet state ET (solid line). The dashed line corresponds to the reorganization energy and H_{DA} values calculated for PC1 in the extended conformation.

Triplet excited-state ET quenching rates (see Table 1 and Figure 2) for PC0, PC1-tBu, PC1, and PC1-Am are 4 orders of magnitude smaller than the corresponding rates from the singlet excited states. This difference is much larger than is expected from the 0.5 eV difference in reaction driving force between the singlet and triplet excited-state systems, assuming that the reorganization energy is ∼1.0 eV. This observation suggested to the authors of refs 6−8 that the electronic coupling element for the singlet and triplet processes must differ by 1 or 2 orders of magnitude in absolute value. The similar large apparent difference between triplet and singlet ET rates was observed for PC0, which lacks the methyl bridging group of PC1.

In sharp contrast with PC0 and the PC1-*x* series, the PC2 and PC3 species with longer and somewhat more flexible linkers display a considerably smaller difference between singlet and triplet ET rates (∼2 orders of magnitude). This observation suggested that the electronic matrix elements in these systems must depend relatively *weakly* on the donor spin state.

Another puzzling aspect of ET in these molecules is that the observed rates increase with increasing linker length (e.g., ET in PC2 is faster than in PC1). The authors attributed this effect to the symmetry of the electronic wave functions that might cause anomalous electronic coupling in the single methylene unit (PC1-*x*) series. This puzzling mixed dependence upon spin state and linker length motivated the theoretical investigation described here.

In summary, the original interpretation of the experimental ET rates of Table 1 was (i) reorganization energies in the compounds studied are ∼1.0 eV, because the observed PC1-Am singlet ET rate is smaller than that in singlet PC1; (ii) PC0, PC1, PC1-tBu, and PC1-Am have at least 1 order of magnitude smaller donor−acceptor coupling in the triplet than in the singlet

(9) Marcus, R. A. *Annu. Rev. Phys. Chem.* **1964**, *15*, 155−196.
(10) Closs, G. L.; Calcaterra, L. T.; Green, N. J.; Penfield, K. W.; Miller, J. R. *J. Phys. Chem.* **1986**, *90*, 3673−3683.
(11) Miller, J. R.; Beitz, J. V.; Huddleston, R. K. *J. Am. Chem. Soc.* **1987**, *109*, 5061−5065.
(12) Closs, G. L.; Miller, J. R. *Science* **1988**, *240*, 440−447.
(13) Gould, I. R.; Ege, D.; Mattes, S. L.; Farid, S. *J. Am. Chem. Soc.* **1987**, *109*, 3794−3796.
(14) Gould, I. R.; Moser, J. E.; Ege, D.; Farid, S. *J. Am. Chem. Soc.* **1988**, *110*, 1991−1993.
(15) Gould, I. R.; Moody, R.; Farid, S. *J. Am. Chem. Soc.* **1988**, *110*, 7242−7244.
(16) Gould, I. R.; Moser, J. E.; Armitage, B.; Farid, S.; Goodman, J.; Herman, M. *J. Am. Chem. Soc.* **1989**, *111*, 1917−1919.

excited donor state; (iii) PC1, PC1-Am, and PC1-tBu have anomalously small electronic couplings in the singlet excited state compared to the corresponding two (PC2) and three (PC3) methylene unit systems, because of a bridge symmetry effect; (iv) donor−acceptor communication is dominated by through-bridge rather than through-space interactions. Our theoretical analysis of these ET systems caused us to revise this interpretation considerably.

We have used a hybrid theoretical approach employing a number of modern methods to analyze the factors that control ET in these iridium−spacer−pyridinium systems. Our results provide a reinterpretation with the following key qualitative features: (i) It is critical to account for the flexibility of these compounds in the theoretical analysis. ET in compounds with more flexible linkers (PC2 and PC3) is *dominated* by the subpopulation of "folded" conformations that have large donor−acceptor contact interactions, and relatively small reorganization energies (∼1.3 eV). The lower probability of folding in the PC3 structure compared to the PC2 structure is the main reason that PC3 has a smaller ET rate than PC2. (ii) The PC1, PC1-Am and PC1-tBu species, although they also exhibit transitions between multiple conformations, do not fold with the pyridinium as close to the iridium donor as in PC2. A larger average reorganization energy, smaller electronic coupling, and smaller rate constant are all expected in these three species than in PC2. (iii) We calculated the reorganization energies for the unfolded conformations of these compounds to be quite large (>1.6 eV) because of the large outer-sphere reorganization energy. Reorganization energies in the folded PC2 and PC3 conformations are smaller by 0.3−0.4 eV. PC1, PC1-Am, and PC1-tBu have reorganization energy smaller by 0.2−0.3 eV in their folded conformations than in their more dominantly populated extended conformations. (iv) The large reorganization energy in the PC0 and PC1-*x* series is the dominant reason for the large observed difference between triplet and singlet excited state ET rates, although electronic coupling is calculated in some cases (see Table 2) to be smaller by a factor of 2 in the triplet states compared to the singlet states. (v) The low ET rate observed from the singlet excited state of PC1-Am (compared to PC1) is explained by a combination of two factors: (a) PC1-Am persists in the extended conformation on the time scale of the ET reaction and (b) PC1-Am has an anomalously small donor−acceptor electronic coupling element in the extended conformations, attributed to interference between competing electron and hole tunneling pathways.

The plan of this paper is as follows. Section II provides a *qualitative* theoretical analysis of the experimental data, outlining the main features of this new interpretation. Section III describes the molecular dynamics simulation of the flexible molecules and the analysis of molecular conformations. Section IV describes the reorganization energy calculations based on numerical solution of the Poisson−Boltzmann equation. Section 5 describes the electronic tunneling matrix element and the ET rate calculations. Finally, Section VI discusses the results of this hybrid analysis.

II. Qualitative Theoretical Analysis

Before we describe detailed numerical calculations of ET rates in the linked iridium/pyridinium molecules, we will describe relatively simple empirical estimates of the reorganization energies and coupling elements in these systems. These simple estimates provide a general qualitative framework for understanding the experimental rates, and motivate the more detailed calculations.

First, we estimate the donor−acceptor electronic coupling using a pathway model.[17] In this simple formulation, through-bridge donor−acceptor electronic coupling is expressed as

$$H_{DA} = H^0_{DA} \exp[-\beta(N-1)] \qquad (2.1)$$

where N is the number of covalent bonds in the molecular bridge connecting donor and acceptor. Experiments and theory show that the typical decay per bond in hydrocarbon model systems is about 0.6.[17] A typical value for the "contact" interaction H^0_{DA} is about 0.1 eV.[18] Using these simple parameters, the D−A couplings in PC0, PC1, PC2, and PC3 would be 8×10^{-3}, 5×10^{-3}, 3×10^{-3}, and 2×10^{-3} eV, respectively. This simple prescription, which has been used extensively in the literature, does not introduce different decay or prefactor parameters for singlet and triplet ET. In the Appendix, we show that providing the spatial electronic distributions in the singlet and triplet excited donor states are similar (likely for the Ir_2−pyrazolyl complexes), we do not anticipate large differences in either the direct or bridge mediated coupling interactions for the two states.

The donor−acceptor electronic coupling elements extracted from experiment (assuming a reorganization energy $\lambda = 1$ eV) for PC0, PC1, PC2, and PC3 were[8] 2×10^{-3}, 6×10^{-4}, 3×10^{-3}, and 8×10^{-4} eV for singlet excited-state electron transfer and 4×10^{-5}, 3×10^{-5}, 3×10^{-3}, and 8×10^{-4} eV for triplet excited-state ET. The singlet couplings extracted from experiment are 1 order of magnitude smaller than the pathway estimates. The triplet couplings extracted from the experiment are 2 orders of magnitude smaller than the pathway estimates. While this level of "theory" is approximate, it is unlikely to be wrong by 2 orders of magnitude. As such, we suspect that the earlier analysis assuming $\lambda \approx 1$ eV underestimated the donor−acceptor electronic interactions.

Several studies of small molecules (and proteins), comparing triplet vs singlet excited-state ET reactions, have been reported.[18−20] In some cases, differences in triplet versus singlet ET rates—not arising simply from reaction free energy differences—were observed. These rate differences can be attributed to geometrical distortions of the excited triplet state that result in an increased inner-sphere reorganization energy. In contrast, the 4 order of magnitude rate difference for triplet versus singlet ET in the donor−acceptor compounds discussed here was attributed largely to differences in electronic coupling.[6,8] If geometrical distortion of the donor in the triplet state were responsible for the observed difference in singlet and triplet ET rates in PC0, PC1, PC1-Am, and PC1-tBu compounds, we would have expected the same low triplet ET rate constant for PC2 which is two orders of magnitude larger than for PC1 (see Table 1).

To explain large observed rates in PC2 and PC3 compounds compared to PC0 and PC1 (see Table 1), one could suggest that the longer and more flexible phosphinite ligands of these compounds fold prior to electron transfer, resulting in smaller reorganization energies and larger donor−acceptor electronic coupling.

A qualitative analysis of outer sphere reorganization energy can be made with the Marcus equation, valid for spherical donors and acceptors:

(17) Onuchic, J. N.; Beratan, D. N.; Winkler, J. R.; Gray, H. B. *Annu. Rev. Biophys. Biomol. Struct.* **1992**, *21*, 349−377.

(18) Bowler, B. E.; Raphael, A. L.; Gray, H. B. *Prog. Inorg. Chem.* **1989**, *38*, 259−322.

(19) Turro, N. J. *Modern Molecular Photochemistry*; Benjamin Cummings: New York, 1978.

(20) Caspar, J. V.; Wang, Y. *Chem. Phys. Lett.* **1994**, *218*, 221−228.

$$\lambda_o = e^2 \left(\frac{1}{2r_D} + \frac{1}{2r_A} - \frac{1}{r}\right)\left(\frac{1}{n^2} - \frac{1}{\epsilon_S}\right) \qquad (2.2)$$

Here r_D and r_A are the radii of donor and acceptor, r is the center-to-center distance between donor and acceptor, ϵ_S is the dielectric constant of the solvent, and n is the solvent index of refraction.

We computed the minimum donor−acceptor distance between the Ir_2 and pyridinium centers in the folded conformation to be about $r_{min} = 8.0$ Å, using a computer molecular model for PC2. Assuming that the donor and acceptor are spherical in the contact conformation, one finds $r_D + r_A = r_{min}$. As the Ir_2 donor is larger than the pyridinium acceptor, we set $r_D = 5.0$ Å and $r_A = 3.0$ Å. Equation 2.2 for this contact geometry gives $\lambda_o = 1.07$ eV. In the extended conformation of PC2, the center-to-center donor−acceptor distance is about $r_{max} = 13.0$ Å. The corresponding Marcus formula for reorganization energy gives $\lambda_o = 1.48$ eV. These simple estimates of the outer sphere reorganization energy show that the reorganization energies of the flexible compounds in the folded vs extended conformations should differ by about 0.4 eV. Hence, the ET rate is expected to be much larger (when $|\Delta G°| < \lambda$) in the compact than in the extended configuration. ET in molecules with fluctuating bridges has recieved recent attention.[21,22]

Geometrical constraints in the more rigid PC0, PC1, PC1-tBu, and PC1-Am compounds presumably force larger distances than in compact PC2 compounds (greater than 10 Å center-to-center) between donor and acceptor groups, causing the total reorganization energies in these compounds to be relatively large (greater than 1.5 eV, assuming 0.3 eV inner-sphere reorganization energy). Large average reorganization energies in these compounds compare to the PC2 molecules would explain the observed smaller ET rate constant in PC1 compared to PC2. When $\lambda \gg |\Delta G°|$ the rate dependence on the reaction driving force is steep see Figure 2. This effect could explain the large difference between singlet and triplet ET rates.

In the following sections we support the qualitative arguments sketched above using detailed numerical simulations of the iridium donor−acceptor complexes.

III. Molecular Dynamics Analysis of the Flexible Compounds

Earlier interpretations of ET experiments in PC2 and PC3[5−8] assumed that these flexible molecules remained in an extended conformation. As such, superexchange interactions mediated by the linker, rather than direct donor−acceptor contact interactions, were assumed to dominate the coupling. In section II we argued that although the thermal population of folded conformations could be low, these folded conformations might dominate the ET process because of their substantially smaller reorganization energy (and/or stronger D−A electronic coupling interaction) than in the extended configurations.

To estimate the relative population of the folded states and the time scales for interconversion between folded and extended species, we performed molecular dynamics (MD) simulations on PC1, PC1-Am, PC2, and PC3 compounds in acetonitrile. The acetonitrile solution was described with a box of 512 three-point model molecules[23] with periodic boundary conditions. Atomic coordinates of the Ir_2 core including two $P-Ph_2-O$ ligands were based on the X-ray structure of $[Ir(\mu\text{-pz*})(CO)\text{-}(Ph_2P\text{-}O\text{-}C_6H_4\text{-}CH_3)]_2$[8] and held fixed in the simulations. Amber atom−atom force field parameters[24] were used for most atoms. The van der Waals parameters of Ir were taken to be the same as for Fe in the Amber database. Atomic partial charges were determined from results of CIS calculation using the Merz−Singh−Kollman charge fitting scheme.[25,26] A 3-21G basis set was used on all atoms except iridium, which was modeled with the effective core potentials of Hay and Wadt[27] using a corresponding double-ζ basis set.

Figure 3A shows the distance fluctuations between the pyridinium ring center and the Ir_2 dimer center obtained in the MD simulations of PC2, PC3, PC1, and PC1-Am at room temperature.

All complexes remain in the extended geometry most of the time, with an 11−13 Å separation between Ir_2 and pyridinium. However, from time to time, a conformational transition into a folded state occurs, resulting in a donor−acceptor distance of 8−9 Å.

In typical folded conformations of PC2 and PC3, the pyridinium ring is in van der Waals contact with the pyrazole or carbonyl ligands of the iridium (see Figure 3B). We expect that such folded complexes have a much smaller reorganization energy and larger electronic coupling than in the extended conformation, and this suspicion is confirmed by further electronic structure calculations (see Table 2). Therefore, even though the thermal population of the folded states is smaller than that of the extended states, we expect that the folded geometries will dominate the ET process in PC2 and PC3. In other words, ET reactions in PC2 and PC3 are gated by conformational fluctuations. One can see from Figure 3A that PC2 folds six times in 1500 ps. Taking into account that there are two independent phosphinite ligands in the complex, a 150 ps average folding time results in agreement with the observed lifetime of the iridium excited state, supporting the hypothesis that ET in PC2 is triggered by folding of the phosphinite ligand. Of course, this prediction can be tested by designing ET systems to have varied folding times but (otherwise) similar ET characteristics. Figure 3A shows that the probability of folding PC3 is smaller than that for folding PC2. Thus, we can interpret the lower ET rate in PC3 as arising from the lower thermal population of the folded state.

The PC1 and PC1-Am compounds also show transitions between the extended and folded conformations, although the frequency of conformational transitions in PC1 and PC1-Am is substantially lower than in PC2. The average folding time for PC1 can be estimated from Figure 3A to be about 400 ps. (We take into account the factor of 2 arising from the presence of two phosphinite ligands in the complex.) PC1-Am folds just two times in the 4 ns of MD simulation, so we expect PC1-Am to remain in the extended conformation on the time scale of the singlet state electron transfer reaction.

IV. Poisson−Boltzmann Calculation of Reorganization Energies

The key new element of the present rate data analysis is the relatively large reorganization energy (>1.3 eV) estimated for the set of compounds PC1, PC1-Am, and PC1-tBu. Recall that a reorganization energy of about 1 eV was assigned in previous studies because of the slower ET rate in PC1-Am compared to that in PC1.[5−8]

(21) Wolfgang, J.; Risser, S. M.; Priyadarshy, S.; Beratan, D. N. *J. Phys. Chem. B* **1997**, *101*, 2986−2991.
(22) Daizadeh, I.; Medvedev, E. S.; Stuchebrukhov, A. A. *Proc. Natl. Acad. Sci. USA* **1997**, in press.
(23) Bohm, H. J.; McDonald, I. R. *Mol. Phys.* **1983**, *49*, 347−360.
(24) Pearlman, D. A.; Case, D. A.; Caldwell, J. W.; Ross, W. S.; Cheatham, T. E., III; Ferguson, D. M.; Seibel, G. L.; Singh, U. C.; Weiner, P. K.; Kollman, P. A. *AMBER 4.1*; University of California: San Francisco, 1995.
(25) Singh, U. C.; Kollman, P. A. *J. Comput. Chem.* **1984**, *5*, 129−145.
(26) Besler, B. H.; Merz, K. M.; Kollman, P. A. *J. Comput. Chem.* **1990**, *11*, 431−439.
(27) Hay, P. J.; Wadt, W. R. *J. Chem. Phys.* **1985**, *82*, 299−310.

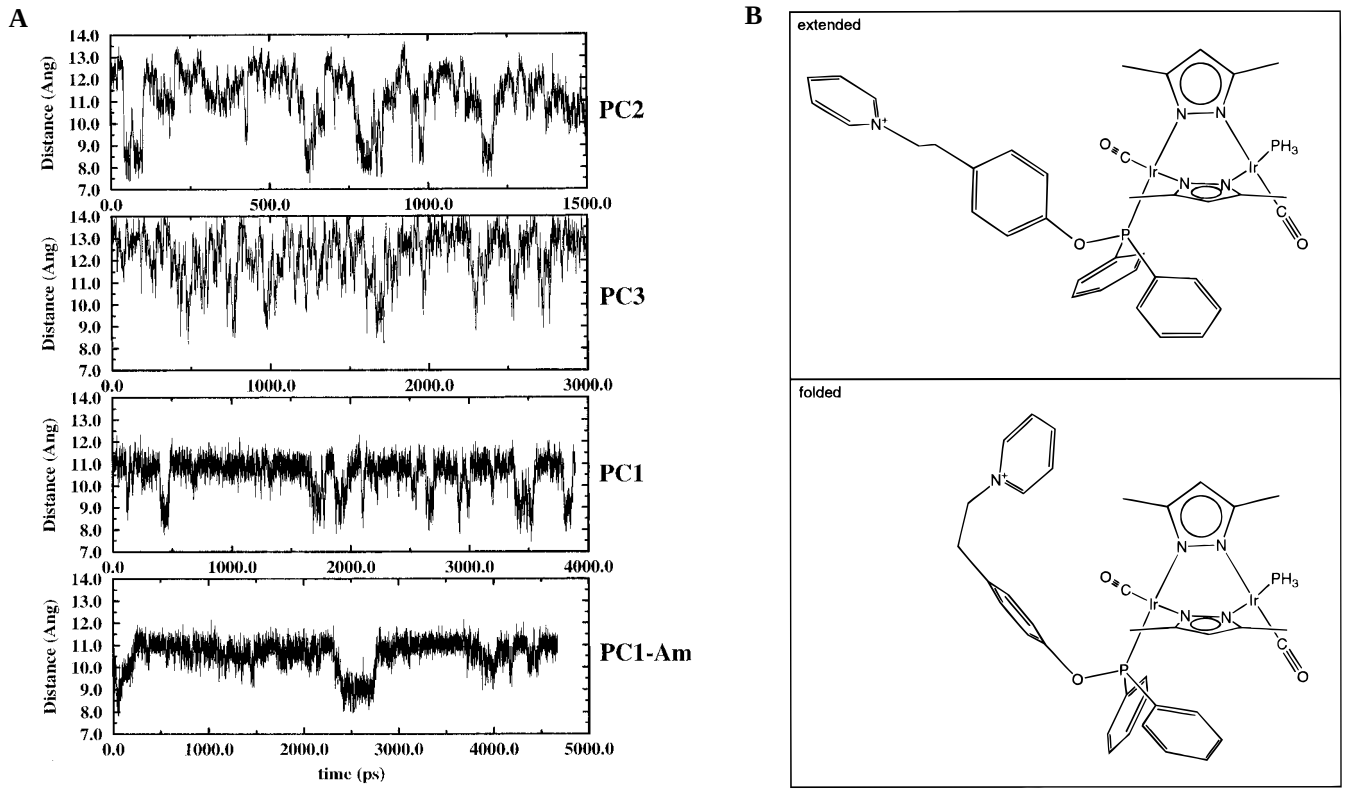

Figure 3. (A) Time dependence of the distance between centers of the iridium dimer and the pyridinium groups in the MD simulation of PC2, PC3, PC1, and PC1-Am, and (B) typical extended and folded configurations of PC2 taken from the MD simulation.

The electron-transfer reorganization energy arises from changes in the equilibrium geometries of the redox species (inner-sphere reorganization energy) and changes in solvent dielectric displacement[1] (outer-sphere reorganization energy) when an electron is transferred from donor to acceptor.

The outer-sphere reorganization energy can be computed as[28,29]

$$\lambda_o = F(\Delta\rho,\epsilon_\infty) - F(\Delta\rho,\epsilon_0) + F_{\text{prom}} \qquad (4.1)$$

$\Delta\rho$ is the electron density change of the solute upon ET. $F(\Delta\rho,\epsilon_\infty)$ and $F(\Delta\rho,\epsilon_0)$ are the free energies of the system with charge density on the solute equal to $\Delta\rho$ and solvent dielectric constant equal to ϵ_∞ (optical dielectric constant) and ϵ_0 (static dielectic constant) respectively. F_{prom}, the promotional energy, is the difference in the electronic energies of the donor and acceptor associated with the change in electron density of the solute that occurs when the solvent relaxes from its equilibrium configuration in the initial state to the equilibrium configuration of the final state. To make a rough estimate of F_{prom}, we performed Hartree−Fock calculations on PC1 with surrounding point charges chosen to model the solvation of the complex in the initial and final electronic states. F_{prom} is computed to be less than 0.1 eV. In the following analysis we disregard F_{prom} in the reorganization energy computation.

In the last few years, models based on a continuum representation of the solvent have been very successful in estimating solvation energies[30] and related quantities including redox potentials.[31] These methods are based upon finite-difference solutions of the Poisson−Boltzmann equation (FDPB) for the electrostatic potential in the medium divided into regions with different dielectric constants. The solvent is modeled as a dielectric continuum with a dielectric constant equal to the experimental value ($\epsilon_0 = 37$ for MeCN). The solute is represented by a cavity of lower dielectric constant ($\epsilon_\infty = 1.8$ to account for electronic polarizability). The boundary between solute and solvent regions is generated by rolling a sphere representing a solvent molecule along the van der Waals surface of the solute. All points outside of the probe surface belong to the solution.

The van der Waals radii of the solute and solvent molecule atoms are parameters of the model. The estimated relative error for a calculated solvation energy in water for both charged and neutral compounds is less than 10% if an optimized set of atomic radii (PARSE) is used.[30] Specifically, atomic radii in this set are the following: $R_C = 1.7$ Å, $R_H = 1.0$ Å, $R_O = 1.6$ Å, and $R_N = 1.5$ Å. The radius of a water molecule is taken as 1.4 Å in these calculations. The outer-sphere reorganization energy appears in eq 4.1 as a difference of solvation energies, so we can use dielectric continuum models to calculate this quantity and expect the same error (of about 10%) in outer-sphere reorganization energy as for calculations of the solvation energies. Calculations of this kind were performed for model ET systems recently.[29]

We expect solute atomic radii and solvent probe radius parameters to be larger for acetonitrile than for water because of its larger size. We assign a solvent radius of 2.5 Å on the basis of the calculated volume of an acetonitrile molecule (63.4 Å^3 from Hartree−Fock calculations). Solvent atomic radii were adjusted in the following manner. We began with PARSE radii and increased the radii to match experimental redox potentials in acetonitrile and ionization potentials for the series of compounds. We used the following formula to relate redox

(28) Marcus, R. A. *J. Chem. Phys.* **1956**, *24*, 966−978.
(29) Liu, Y. P.; Newton, M. D. *J. Phys. Chem.* **1995**, *99*, 12382−12386.
(30) Sitkoff, D.; Sharp, K. A.; Honig, B. *J. Phys. Chem.* **1994**, *98*, 1978−1988.
(31) Zhang, L. Y.; Friesner, R. A. *J. Phys. Chem.* **1995**, *99*, 16479−16482.

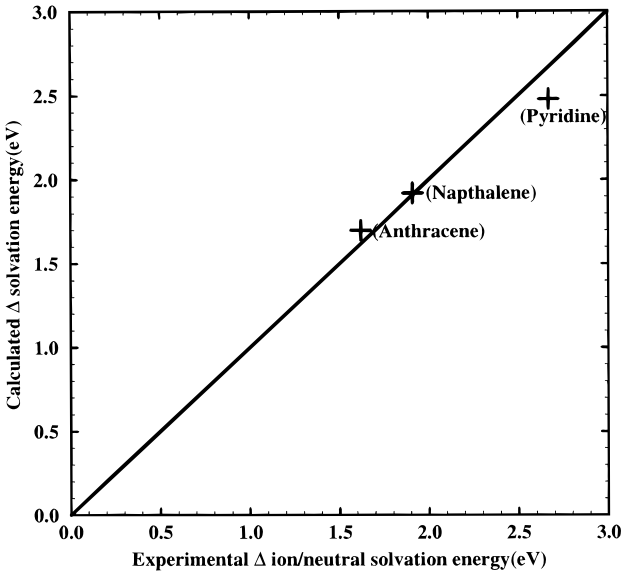

Figure 4. Correlation between differences of solvation energies in the neutral molecules and their ions (in acetonitrile) calculated from the experimental ionization potentials, electronic affinities, and the reduction/oxidation potentials using eq 4.2; and the same quantities calculated using the FDPB method.

potentials and ionization potentials:[31]

$$IP = 4.7 \text{ eV} + eE_{ox} + [E_{solv}(\text{cation}) - E_{solv}(\text{neutral})] \quad (4.2)$$

where IP is the ionization potential of a molecule in electronvolts, E_{ox} is the oxidation potential vs SCE (V), and $[E_{solv}(\text{cation}) - E_{solv}(\text{neutral})]$ is the difference in solvation energies of cation and neutral molecules.

Figure 4 shows the correlation between the solvation energy difference $[E_{solv}(\text{cation}) - E_{solv}(\text{neutral})]$ calculated from eq 4.2 using experimental oxidation and ionization potential values and the same quantity calculated with the FDPB method using the adjusted set of atomic radii parameters ($R_C = 2.0$ Å, $R_H = 1.2$ Å, $R_O = 1.6$ Å, $R_N = 1.7$ Å) that we used further to calculate the reorganization energies of the iridium complexes. The radii of the iridium and phosphorus atoms were determined from calculations of the volumes of isolated Ir and P atoms. These calculations gave $R_{Ir} = 2.3$ Å and $R_P = 2.1$ Å. Similar calculations on carbon and hydrogen atoms gave $R'_C = 1.8$ Å and $R'_H = 1.4$ Å, differing by 0.2 Å from the values obtained by adjusting the atomic radii to the difference in solvation energies of cation and neutral reference molecules. The uncertainty of ±0.2 Å in atomic radii for Ir and P translates into less than 2% variation in the calculated reorganization energy of the iridium complexes, acceptable because the expected accuracy of these calculations is about 10%.

Atomic charges and dielectric boundary conditions were mapped onto a rectangular grid of 121 × 121 × 121. Atomic charges were obtained using the Singh−Merz−Kollman charge-fitting scheme[25,26] with Hartree−Fock and CIS calculations on the donor and acceptor groups (the same strategy was used to obtain atomic charges for the MD simulations) (see section III). Electrostatic potentials at grid points were computed numerically by solving the Poisson equation:

$$\vec{\nabla}\epsilon(\vec{r})\cdot\vec{\nabla}\phi(\vec{r}) + 4\pi\rho(\vec{r}) = 0 \quad (4.3)$$

Finally, the reorganization energy was computed using the electrostatic potentials.

We used the DelPhi program[32] to compute the electrostatic potentials. In analogy with expressions for electrostatic solvation energies,[30] the outer-sphere reorganization energy was calculated as

$$\lambda_o = \frac{1}{2}\sum_i \Delta q_i^{DA}(\phi_i^{\epsilon_0} - \phi_i^{\epsilon_\infty}) \quad (4.4)$$

where Δq_i^{DA} is the change in the electron density at a grid point when the electron is transferred from donor to acceptor. $\phi_i^{\epsilon_0}$ and $\phi_i^{\epsilon_\infty}$ are the electrostatic potentials calculated at the grid points with the charge distribution given by Δq_i^{DA} and the solvent dielectric constant equal to the solvent static and optical dielectric constant, respectively.

To estimate the inner-sphere reorganization energy, we performed geometry optimization of the isolated donor and acceptor species in the oxidized and reduced states using *ab initio* calculations. We truncated the donor group, substituting phosphinite ligands with PH_3 groups. The acceptor was modeled by an *N*-methylpyridinium compound. Changes in the pyridinium geometry were computed at the MP2 level (Møller−Plesset second-order correlation energy corrections[33,34]) using a 6-31G(d) basis set. The geometry of the iridium donor (with phosphinite ligands truncated to PH_3) in the excited state was calculated with the CIS (single excitation configuration interactions (CI)) method in a 3-21G basis set and with the Hartree−Fock method using the same basis set for the oxidized state. Effective core potentials and a corresponding double-ζ basis set[27] were used for the iridium atoms. The inner-sphere reorganization energy was calculated from the difference in energies of the redox groups in the equilibrium geometries of the two oxidation states. We found the contribution of the pyridinium group to the inner-sphere reorganization energy to be approximately 0.2 eV and that of the iridium dimer donor to be 0.1 eV, resulting in a total inner-sphere reorganization energy of about 0.3 eV (in agreement with previous estimates[8]). The difference between the equilibrium geometries of the Ir_2 donor in the triplet and singlet states was found to be small.

The sum of the calculated outer- and inner-sphere reorganization energies for the different iridium complexes in distinct conformations are given in Table 2. The FDPB calculational results support the qualitative arguments of section II, suggesting a substantial dependence of the reorganization energy on donor−acceptor complex geometry.

Figure 5 shows the time dependence of the outer-sphere reorganization energy calculated at various points in the MD trajectories for PC1, PC1-Am, PC2, and PC3. Comparing Figures 5 and 3, one sees that decreasing the donor−acceptor distance decreases the calculated reorganization energy. Figure 7 shows that there exists a strong linear correlation between the calculated outer-sphere reorganization energy and the inverse donor−acceptor distance, as anticipated by the Marcus formula, eq 2.2.

V. Calculation of Donor−Acceptor Electronic Coupling and ET Rate Constants

Numerical estimates of tunneling matrix elements are essential for calculating nonadiabatic ET rates. However, reliable calculations of this electronic property remain a considerable challenge despite much recent progress.[3] In the calculations

(32) Nicholls, A.; Sharp, K. A.; Honig, B. *DelPhi V3.0*; Department of Biochemistry and Molecular Biophysics, Columbia University: New York, 1990.

(33) Møller, C.; Plesset, M. S. *Phys. Rev.* **1934**, *46*, 618−622.

(34) Head-Gordon, M.; Pople, J. A.; Frisch, M. J. *Chem. Phys. Lett.* **1988**, *153*, 503−506.

Table 2. Theoretical Values of ET Parameters and Rates (S = Singlet, T = Triplet) in Ir_2−(Bridge)−Pyr^+ Compounds

compound	conformation	H_{DA} (eV) S/T[a]	λ (eV)	$-\Delta G°$ (eV) S/T[a]	k_{ET} (s^{-1}) S/T
PC0		0.02/0.01	1.65	0.80/0.30	$7.4 \times 10^{10}/2.8 \times 10^{7}$
PC1-tBu	extended	0.02/0.02	1.7	0.43/-0.07	$5.1 \times 10^{8}/8.4 \times 10^{4}$
	folded	0.01/0.01	1.4	0.43/-0.07	$1.3 \times 10^{8}/4.2 \times 10^{5}$
PC1	extended	0.01/0.005	1.7	0.66/0.16	$2.6 \times 10^{9}/4.1 \times 10^{5}$
	folded	0.01/0.01	1.4	0.66/0.16	$3.2 \times 10^{10}/3.2 \times 10^{7}$
PC1-Am	extended	0.002/0.002	1.7	1.06/0.56	$4.9 \times 10^{9}/3.0 \times 10^{7}$
	folded	0.01/0.005	1.4	1.06/0.56	$6.0 \times 10^{11}/2.0 \times 10^{10}$
PC2	extended	0.006/0.006	1.8	0.57/0.07	$1.2 \times 10^{8}/4.3 \times 10^{4}$
	folded	0.02/0.02	1.3	0.57/0.07	$1.1 \times 10^{11}/7.1 \times 10^{7}$
PC3	extended	0.003/0.003	1.8	0.59/0.09	$4.1 \times 10^{7}/1.55 \times 10^{4}$
	folded	0.01/0.01	1.3	0.59/0.09	$3.3 \times 10^{10}/9.4 \times 10^{6}$

[a] Computed couplings are ±50% from computation using the modified Hartree−Fock IVO method, fragment method, and direct CIS calculations (for PC0, PC1, and PC2). [b] The ΔG values are shifted 0.1 eV compared to Table 1, as explained in the text.

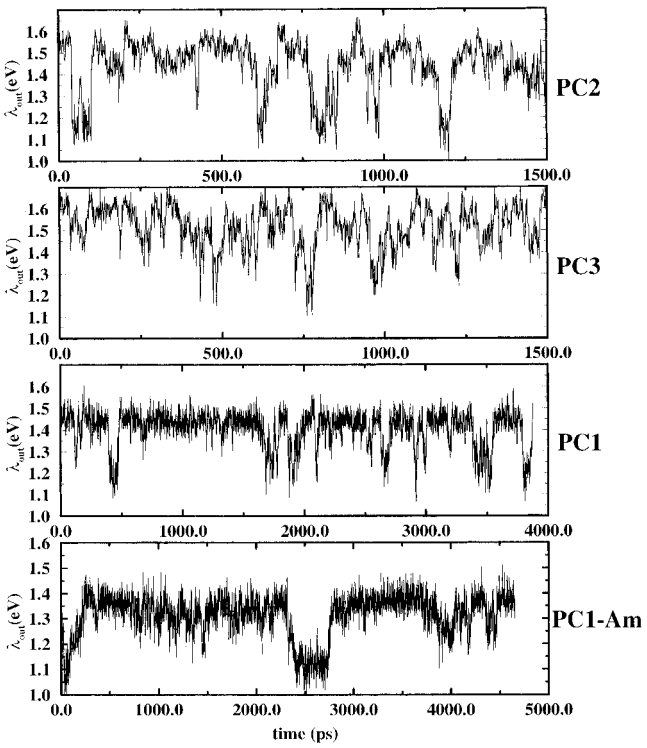

Figure 5. Time dependence of the outer-sphere reorganization energies for PC2, PC3, PC1, and PC1-Am calculated using the FDPB method at points along the MD trajectory.

reported here, we used an effective valence Hamiltonian approach described elsewhere,[35] as well as conventional *ab initio* electronic structure methods, to calculate the electronic matrix elements in the donor−acceptor molecules.

In order to compute the electronic coupling, we construct the effective one-electron Hamiltonian of the system first. We build this Hamiltonian in two different ways. One strategy is to perform a Hartree−Fock calculation on the full donor−bridge−acceptor system. To make this calculation possible, we truncate all the atom groups that are not directly involved in mediating donor−acceptor coupling or essential for the electronic structure of the donor. Figure 8 shows the truncated structure. A second strategy that we also used was to construct the effective Hamiltonian via a "divide and conquer" strategy.[35] We perform several Hartree−Fock calculations on the molecular fragments of the system shown in Figure 8. We assembled a composite valence effective Hamiltonian from the fragment Hamiltonians.[35] The advantage of the latter approach is that we can use larger basis sets in the fragment calculations and include the atom groups that were eliminated in the direct calculations. A split valence 3-21G basis was used in the direct Hartree−Fock calculations of the donor−bridge−acceptor complexes for all atoms except iridium. Iridium atoms were modeled with the effective core potentials of Hay and Wadt,[27] and a corresponding double-ζ basis set. The outermost core electrons are included in the active space in this pseudopotential scheme.[27] Fragment calculations were performed with 3-21G and 3-21+G basis sets. Results obtained by the direct and by the fragmentation methods were within 30% of each other.

We are examining excited-state electron transfer. The Fock operator obtained in standard Hartree−Fock calculations provides a poor description of excited states because the unoccupied orbitals "feel" the electrostatic repulsion of all N-electrons in the system. This is more appropriate for the description of anionic states[36] than it is for excited electronic states. To obtain an effective one-electron Hamiltonian for the system that provides a better description of the excited states, we used the IVO (improved virtual orbital) method.[37,38] In this strategy the Fock operator matrix of the system is modified so the effective potential acting on unoccupied orbitals corresponds to the effective potential of the electron excited from a particular occupied orbital provided the occupied orbitals are not changed when the electron is excited.

For singlet excitation from the *i*-th occupied orbital, the expression for the modified Fock operator matrix is[38]

$$\mathbf{F}' = \mathbf{F} - \mathbf{Q}(\mathbf{J}_i - \mathbf{2K}_i)\mathbf{Q} \tag{5.1}$$

while for triplet excitation the appropriate modified Fock operator matrix is

$$\mathbf{F}' = \mathbf{F} - \mathbf{Q}\mathbf{J}_i\mathbf{Q} \tag{5.2}$$

Here **F** is the Fock matrix of the system, F′ is the modified Fock matrix, **Q** is the matrix representation of the projection operator for unoccupied molecular orbitals, and $\mathbf{J}_i$ and $\mathbf{K}_i$ are the coulomb and exchange matrices for the occupied orbital from which the electron is excited. We expect the IVO method to provide a reasonable description of an excited state if this state can be well described by a one-electron excitation from a particular occupied orbital.

A qualitative molecular orbital treatment of the d^8−d^8 iridium dimer complex[39−41] predicts a HOMO that is dominantly dσ* in character, formed from the antisymmetric combination of

(35) Kurnikov, I. V.; Beratan, D. N. *J. Chem. Phys.* **1996**, *105*, 9561−9573.
(36) Jørgenson, P. D. *Second Quantization-Based Methods in Quantum Chemistry*; Academic Press: New York, NY, 1981.
(37) Huzinaga, S.; Arnau, S. *Phys. Rev. A* **1970**, *1*, 1285−1288.
(38) Huzinaga, S.; Arnau, S. *J. Chem. Phys.* **1971**, *54*, 1948−1951.
(39) Smith, D. C.; M., M. V.; Mason, W. R.; Gray, H. B. *J. Am. Chem. Soc.* **1990**, *112*, 3759−3767.

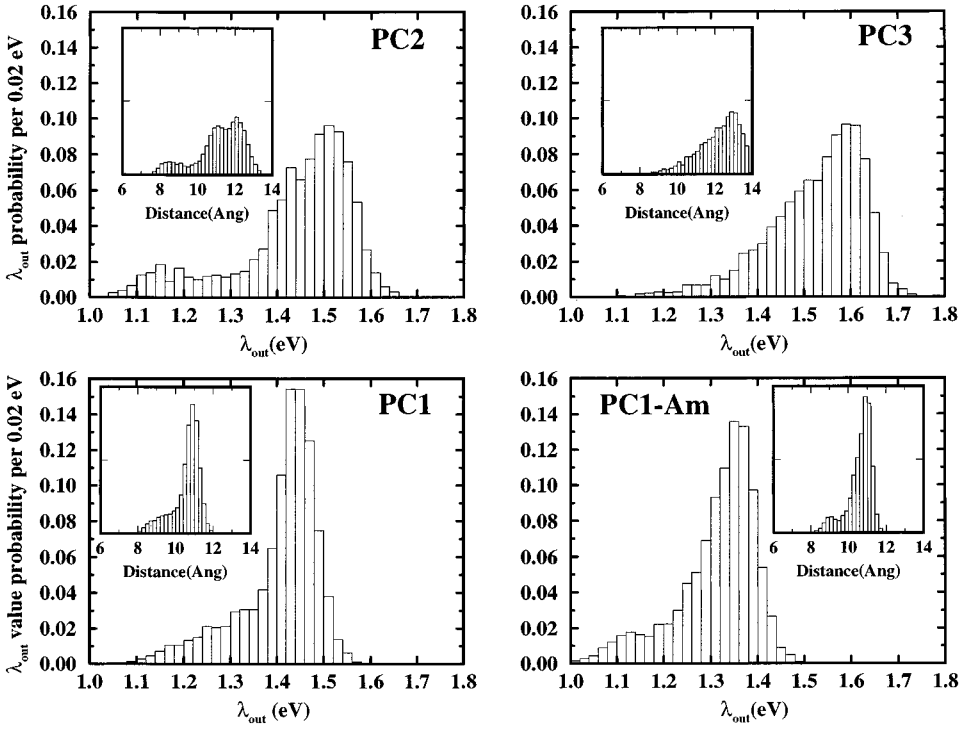

Figure 6. Probability distributions of outer-sphere reorganization energies for PC2, PC3, PC1, and PC1-Am calculated with the FDPB method. The inserts show probability distributions of donor−acceptor distances.

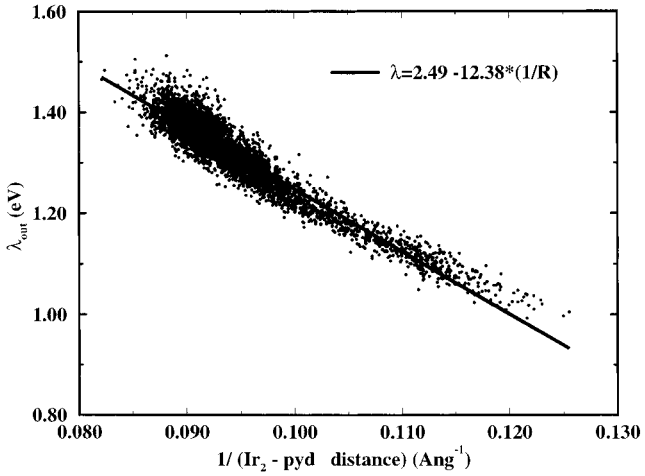

Figure 7. Linear correlation between the inverse donor−acceptor distance in PC1-Am and the FDPB calculated outer-sphere reorganization energy.

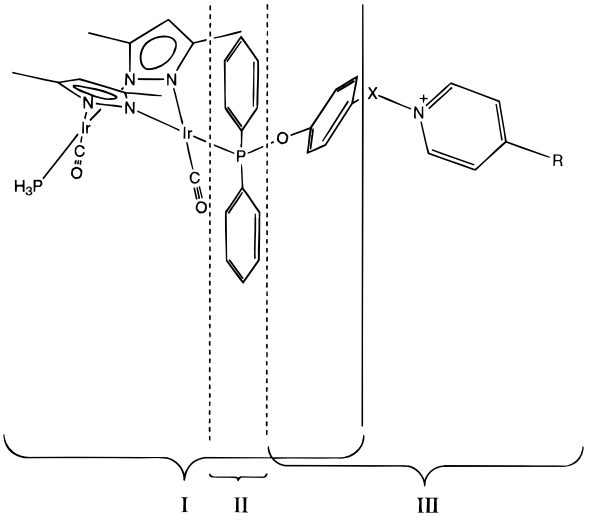

Figure 8. Truncated structures of the donor−acceptor complexes used in the electronic coupling calculations. Brackets show molecular fragments used for electronic coupling calculations in the fragmentation approach. In the direct calculations of the electronic coupling, the phenyl groups at phosphorus were replaced with hydrogen atoms.

iridium d_{z^2} orbitals. The LUMO has mostly pσ character, arising from a symmetrical combination of iridium p_z orbitals. We performed excited states calculations on the iridium complex (with phosphonite ligands truncated to PH_3) using single excitation configuration interaction methods (CIS). These calculations showed that the lowest excited state (for both the singlet and triplet) is dominated by the HOMO → LUMO configuration (the expansion coefficient for this configuration is greater that 0.6). This justifies the use of a one-electron description for the excited state of the complex. The HOMO and LUMO of the Ir_2 donor are shown in Figure 9.

Once the effective Hamiltonian of the system is constructed, we modify it by "shifting" the donor and acceptor energies using eq 5.3 to minimize the energy splitting between donor/acceptor centered eigenstates:

$$\hat{F}(\epsilon_D,\epsilon_A) = \hat{F}_0 + |D\rangle\epsilon_D\langle D| + |A\rangle\epsilon_A\langle A| \qquad (5.3)$$

Here F_0 is the valence space effective Hamiltonian obtained from direct Hartree−Fock calculations of the donor−bridge−acceptor system or from the fragment strategy. $|D\rangle$ and $|A\rangle$ are donor and acceptor molecular orbitals that are obtained by truncating the corresponding eigenstates of the effective Hamiltonian to be localized only on the donor and acceptor groups.

The donor−acceptor coupling was assumed equal to one-half of this minimized splitting. Systematically varying ϵ_D and adjusting ϵ_A to minimize the energy splitting of the donor/

(40) Marshall, J. L.; Hopkins, M. D.; M., M. V.; Gray, H. B. *Inorg. Chem.* **1992**, *31*, 5034−5040.
(41) Lichtenberger, D. L.; Copenhaver, A. S.; Gray, H. B.; Marshall, J. L.; Hopkins, M. D. *Inorg. Chem.* **1988**, *27*, 4888−4893.

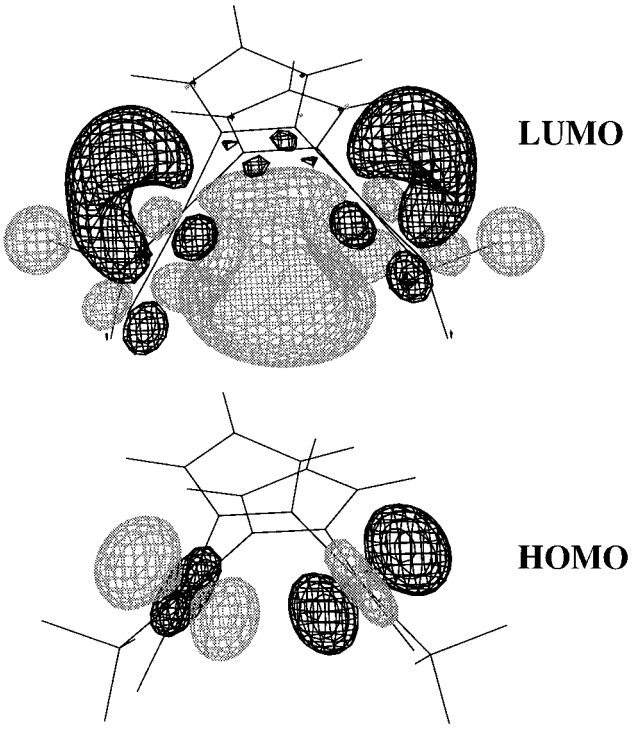

Figure 9. HOMO and LUMO of the Ir_2 donor. Note that the HOMO is dominantly an antisymmetric combination of Ir d_{z^2} orbitals. The LUMO is largely a symmetric combination of Ir p_z orbitals.

acceptor centered eigenstates, we can map out the energy dependence of the electronic coupling.

We performed CIS calculations (in the 3-21G basis set) of the couplings in the PC0, PC1, and PC2 compounds for the extended configurations in both spin states. To compute the donor−acceptor coupling, we minimized the energy splitting between the first two excited states. These two states correspond to donor and acceptor states active in the ET process. The energy levels were shifted by introducing artificial charges around the Ir_2 donor. The results of these donor−acceptor coupling calculations are within 50% of the values calculated with the IVO or fragment methods.

Results of electronic matrix element calculations for different complexes and conformations are presented in Table 2, together with calculated electron-transfer rates based on eq 1.1.

Errors of ±0.1 eV are associated with estimates of $\Delta G°$, arising dominantly from uncertainty in the excited-state donor redox potential. This redox potential was calculated using ground-state redox potentials, absorption spectra, and emission spectra.[8] We use the lower experimental estimate of $\Delta G°$ in Table 2 because it produces rates that better match experiment. The improved description of the rates using the lower value of $\Delta G°$ may indicate that we have systematically underestimated the reorganization energy by ∼0.1 eV, which is within the uncertainty of our λ calculations.

Calculated singlet electron transfer rates for the dominant extended conformations of PC0, PC1, PC1-tBu, and PC1-Am agree well (within a factor of 3) with the experimentally observed values. Electron transfer in the folded conformations of PC1, PC1-tBu, and PC1-Am is calculated to be very fast. However, because of the low population of folded conformations and the low frequency of transitions between extended and folded conformations for the PC1-*x* series (seen to be $(1-2) \times 10^9\ s^{-1}$ in the MD simulation of PC1 and PC1-Am), ET occurs dominantly in the extended conformations of PC1 and PC1-Am. The ET rate in the extended conformation of PC1-tBu was calculated to be lower than the folding frequency and the

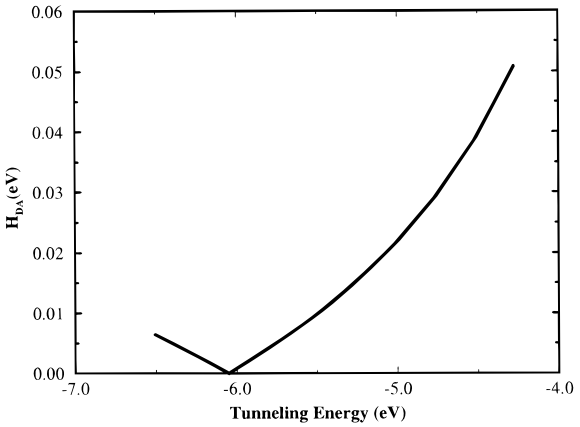

Figure 10. Tunneling energy dependence of the electronic coupling in PC1-Am.

experimental ET rate, which indicates that the folded conformation may contribute to the singlet ET in this molecule.

The triplet rates occur on time scales several orders of magnitude slower than the time scale for interconversion between the folded and extended geometries. Therefore, we expect that the triplet rate constants will be the conformational average of rates in the accessed geometries. In the PC1-*x* species, the population of folded conformations is about 2% (see Figure 6). Triplet rates in PC1 for the extended and folded conformations weighted by their relative populations will give a rate on the order of $10^6\ s^{-1}$, within a factor of 4 of the experimental rate. For the PC1-tBu triplet, the same procedure gives a rate estimate of about $10^5\ s^{-1}$, also consistent with experiment (see Tables 1 and 2).

In PC0, the calculated triplet rate constant is about 30 times faster than observed. The calculated triplet rate for PC1-Am based on the weighted average of the extended and folded configuration rates is about $10^8\ s^{-1}$, 3 orders of magnitude faster than reported in the experiment. The computed rates in both the compact and extended configurations is much faster than observed in the experiment. Descrepencies of this magnitude are well beyond the range of errors that we expect from the uncertainties in the computations. Further experimental and theoretical examination of the origin for this rate difference is needed.

Our findings show that the dramatic differences between triplet and singlet ET rates in the PC0 and PC1 family of compounds arise primarily from the large reorganization energy and the difference in singlet/triplet reaction free energies. This produces a much stronger dependence upon reaction driving force than was anticipated earlier.

The calculated electronic coupling in PC1-Am is much smaller than in PC1 and PC1-tBu. To investigate the origin of this behavior, we calculated the tunneling energy dependence of the electronic coupling in PC1-Am. This was done by systematically varying the donor energy level (changing ϵ_D in eq 5.3) and adjusting the acceptor level (with ϵ_A in eq 5.3) to minimize the energy splitting of donor/acceptor centered eigenstates. Figure 10 shows the tunneling energy dependence of the electronic coupling in PC1-Am. The electronic coupling goes through zero at a tunneling energy value close to the actual binding energy of the PC1-Am acceptor. Additional analysis involving approximate calculations of the coupling using eq 5.4 shows that the zero arises because of cancellation of contributions from unoccupied and occupied bridge localized molecular orbitals (electron and hole contributions) that are of the same magnitude but of different sign:

$$H_{DA}(E) = \sum_{j=1}^{N_{occ}} \frac{(V_{Dj} - E_t S_{Dj})(V_{jA} - E_t S_{jA})}{(E_t - E_j)} + \sum_{j=N_{occ}+1}^{N_{tot}} \frac{(V_{Dj} - E_t S_{Dj})(V_{jA} - E_t S_{jA})}{(E_t - E_j)} \quad (5.4)$$

Here V_{Dj} and V_{jA} are interaction matrix elements between donor and acceptor orbitals and eigenstates of the bridge (which we define here as all eigenstates of the system excluding those built mostly from donor and acceptor orbitals). S_{Dj} and S_{jA} are overlap integrals between donor and acceptor orbitals and eigenstates of the bridge. E_j are the eigenvalues of the bridge, and E_t is the tunneling energy (i.e., the binding energy of the electron in the activated state).

The tunneling energy effects described above for singlet PC1-Am are very sensitive to the estimated tunneling energy. The tunneling energy uncertainty in our calculations is about $\pm$1eV, larger than the width of the dip in the donor−acceptor coupling vs tunneling energy (see Figure 10). Additional studies of rate dependence upon tunneling energy are needed to probe this anomaly further.

Table 2 shows that the ET rates in the folded conformations of PC2 and PC3 are very fast. Thus, the ET rate is limited by the folding process itself; the reaction is gated. In section III we estimated that the folding time for PC2 is about 100 ps and that the folding time for PC3 is about 500 ps, which is in agreement with the measured singlet ET rate constants.

The conformation weighted rates of triplet ET in PC2 and PC3 should be about 10^7 s^{-1} and 10^6 s^{-1} (based on the data of Table 2 and about a 10% population of folded conformations), respectively, an order of magnitude smaller than observed. This may indicate, for example, an underestimation of the electronic coupling in the the folded conformations of PC2 and PC3.

VI. Conclusions

Modern theoretical analysis of electron transfer rates in iridium donor−acceptor systems provides a rich and qualitatively new interpretation for a considerable body of rate data.[6−8] It is important to point out that a hybrid approach, employing MD, electronic structure, and electrostatic calculations, is essential to understand these semirigid systems.

More specifically, we have estimated the solvent reorganization energy and electronic coupling elements for the rigid compounds PC0, PC1, PC1-tBu, and PC1-Am to be much larger than was earlier believed.[6−8] The much slower excited triplet state ET rates (compared to ET from the singlet) arise dominantly from the difference in the reaction free energy (different for the singlet and triplet excited donor states), *not* from considerable differences in the electronic coupling element. Larger ET rates in PC2 and PC3, compared to rates in the smaller PC1 system, are found to arise from a "gating" effect in the flexible PC2 and PC3 compounds. In the flexible systems, the ET process is dominated by a "folded" conformation with a relatively small population, a larger coupling matrix element, and a smaller solvent reorganization energy than in the extended geometry. The analysis of the coupling matrix element energy dependence indicates that the lower electron transfer rate in PC1-Am compared to PC1 arises from the proximity of the tunneling energy in these compounds to the point at which the electronic coupling goes through a zero, which arises from the interference between electron and hole mediation mechanisms. Experimental studies in donor−acceptor compounds of this kind, in which the donor and acceptor energies can be varied systematically, will be critical for testing this and the other predictions of the present investigation.

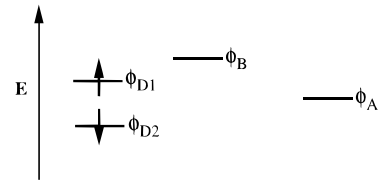

Figure 11. Four-orbital model for excited-state bridge-mediated electron transfer. Shown schematically is the excited donor singlet state.

There are limitations in the accuracy of the theoretical methods used here. For example, empirical force fields that were used in the MD simulations were not fully optimized for these particular molecules. This situation can probably be improved by fitting the parameters to the results of accurate *ab initio* calculations. The calculations of reorganization energy rely upon continuum representations of the solvent. Discrete solvent models could help to remove this intrinsic assumption. Finally, electronic matrix element calculations could be improved by including electron correlation effects, although calculations of this kind are quite costly.

The current analysis demonstrates the prospect for combining *ab initio* electronic structure methods (for computing electronic couplings and inner-sphere reorganization energies), MD methods of examining molecular geometry, and FDPB strategies (for computing outer sphere reorganization energies) to make detailed quantitative predictions of ET rates in rather complex systems. The MD simulations have provided access to the probabilities of obtaining different molecular conformations, and the frequencies of transition between conformations that might result in "gated" ET processes. In the iridium systems examined here, the experimental rates of ET were rather challenging to interpret in the absence of these detailed theoretical considerations. Further comprehensive analysis of this kind can provide feedback that will allow one to address more subtle aspects of ET processes and, in turn, to build improved quantitatively predictive models.

Acknowledgment. We thank the National Science Foundation (Grant CHE-9257093) and the Department of Energy (Grant FE-FG36-94G010051) for support of this research. We thank M. B. Zimmt for proving reference data for calibrating the FDPB calculations and P. J. Hay for providing pseudopotential data. We also thank M. D. Hopkins, V. M. Miskowski, and H. B. Gray for helpful discussions.

Appendix A: Coupling Interactions Involving Singlet vs Triplet States

We show below, using a simple two-electron model, that the effect of spin state on the donor−acceptor electronic coupling should be small provided that the spatial distribution of the singlet and triplet states is similar.

Figure 11 shows schematically a four-orbital two-electron model for excited-state ET mediated by a bridge. Here, we represent donor with two orbitals ϕ_{D1} and ϕ_{D2} (both are singly occupied in the initial state), the acceptor by the orbital ϕ_A, and the bridge by the orbital ϕ_B. This argument can be generalized to include multiple bridge states. The $^1\Psi_D$ and $^3\Psi_D$ (superscripts 1 and 3 define the spin state of the corresponding wave function) are the initial singlet and triplet states. Final charge separated acceptor states are $^1\Psi_A$ and $^3\Psi_A$. The bridge-localized states $^1\Psi_B$ and $^3\Psi_B$ mediate electronic coupling between $^1\Psi_D$ and $^1\Psi_A$, and between $^3\Psi_D$ and $^3\Psi_A$.

The spatial wave functions associated with these states are

$$^3\Psi_D = \frac{1}{\sqrt{2}}[\phi_{D1}(\vec{r}_1)\phi_{D2}(\vec{r}_2) - \phi_{D1}(\vec{r}_2)\phi_{D2}(\vec{r}_1)]$$

$$^3\Psi_A = \frac{1}{\sqrt{2}}[\phi_{D1}(\vec{r}_1)\phi_A(\vec{r}_2) - \phi_{D1}(\vec{r}_2)\phi_A(\vec{r}_1)]$$

$$^3\Psi_B = \frac{1}{\sqrt{2}}[\phi_{D1}(\vec{r}_1)\phi_B(\vec{r}_2) - \phi_{D1}(\vec{r}_2)\phi_B(\vec{r}_1)]$$

$$^1\Psi_D = \frac{1}{\sqrt{2}}[\phi_{D1}(\vec{r}_1)\phi_{D2}(\vec{r}_2) + \phi_{D1}(\vec{r}_2)\phi_{D2}(\vec{r}_1)]$$

$$^1\Psi_A = \frac{1}{\sqrt{2}}[\phi_{D1}(\vec{r}_1)\phi_A(\vec{r}_2) + \phi_{D1}(\vec{r}_2)\phi_A(\vec{r}_1)]$$

$$^1\Psi_B = \frac{1}{\sqrt{2}}[\phi_{D1}(\vec{r}_1)\phi_B(\vec{r}_2) + \phi_{D1}(\vec{r}_2)\phi_B(\vec{r}_1)]$$

The second-order perturbation theory expressions for the direct and superexchange electronic couplings are

$$^iT_{DA-Dir} = {}^iH_{DA} - {}^iE_t{}^iS_{DA} \quad \text{(A1)}$$

$$^iT_{DA-Superex} = \frac{(^iH_{DB} - {}^iE_t{}^iS_{DB})(^iH_{AB} - {}^iE_t{}^iS_{AB})}{^iE_B - {}^iE_t} \quad \text{(A2)}$$

where $i = 1$ or 3 defines the spin multiplicity. $^iH_{DA}$, $^iH_{DB}$, and $^iH_{AB}$ are the Hamiltonian matrix elements between electronic states $^i\Psi_D$, $^i\Psi_A$, and $^i\Psi_B$ respectively. $^iS_{DA}$, $^iS_{DB}$, and $^iS_{AB}$ are overlap integrals between these states. Using the definition of $^3\Psi_D$ and $^3\Psi_A$,

$$^3S_{DA} = \int {}^3\Psi_D\, {}^3\Psi_A \, d\vec{r}_1\vec{r}_2 = \int \phi_{D2}(\vec{r}_1)\phi_A(\vec{r}_1)\, d\vec{r}_1 \quad \text{(A3)}$$

assuming that ϕ_{D1} and ϕ_{D2} are orthogonal. Similarly,

$$^1S_{DA} = \int {}^1\Psi_D\, {}^1\Psi_A \, d\vec{r}_1\vec{r}_2 = \int \phi_{D2}(\vec{r}_1)\phi_A(\vec{r}_1)\, d\vec{r}_1 \quad \text{(A4)}$$

Thus

$$^3S_{DA} = {}^1S_{DA}$$

In the same manner, one finds that

$$^3S_{DB} = {}^1S_{DB}$$

$$^1S_{AB} = {}^1S_{AB}$$

For the Hamiltonian matrix elements

$$\begin{aligned} ^iH_{DA} &= \int {}^1\Psi_D H {}^i\Psi_A d\vec{r}_1\vec{r}_2 \\ &= {}^1/_2\int \phi_{D1}(\vec{r}_1)\phi_{D2}(\vec{r}_2)H\phi_A(\vec{r}_2)\phi_{D1}(\vec{r}_1)\, d\vec{r}_1\, d\vec{r}_2 \\ &\pm {}^1/_2\int \phi_{D1}(\vec{r}_2)\phi_{D2}(\vec{r}_1)H\phi_A(\vec{r}_2)\phi_{D1}(\vec{r}_1)\, d\vec{r}_1\, d\vec{r}_2 \\ &\pm {}^1/_2\int \phi_{D1}(\vec{r}_1)\phi_{D2}(\vec{r}_2)H\phi_A(\vec{r}_1)\phi_{D1}(\vec{r}_2)\, d\vec{r}_1\, d\vec{r}_2 \\ &+ {}^1/_2\int \phi_{D1}(\vec{r}_2)\phi_{D2}(\vec{r}_1)H\phi_A(\vec{r}_1)\phi_{D1}(\vec{r}_2)\, d\vec{r}_1\, d\vec{r}_2 \quad \text{(A5)} \end{aligned}$$

The first and fourth terms on the right hand side in eq A5 are equal, while the second and third terms are zero for a one-electron Hamiltonian H. Thus, for a one-electron Hamiltonian $^3H_{DA} = {}^1H_{DA}$. In a similar manner, one can show that $^3H_{DB} = {}^1H_{DB}$ and $^3H_{AB} = {}^1H_{AB}$.

The singlet−triplet energy splitting of the "bridge" states $^1\Psi_B$ and $^3\Psi_B$ is approximately[42]

$$(^1E_B - {}^3E_B) = H_{DB}H_{DB}/(E_B - E_D) \quad \text{(A6)}$$

We expect $|H_{DB}| \ll 1$ eV and $|E_B - E_D| \gg 1$ eV, so

$$|^1E_B - {}^3E_B| \gg |E_B - {}^iE_t| \quad \text{(A7)}$$

Expressions A1 and A2 thus, to first approximation, differ for the singlet and triplet states only through the tunneling energy parameter ^iE_t.

The tunneling energy dependence of the electronic matrix element is usually smooth far from resonance with bridge localized states, so one expects that electronic coupling elements in the triplet and singlet states will be similar if the electronic distribution is similar in the two spin states. Exceptions may arise when the electronic coupling is anomalously small in one of the spin state because the tunneling energy is close to a zero arising from interference effects. In this case, as discussed in section V, one might expect to find large differences in the electronic coupling associated with singlet vs triplet states.

JA970309R

(42) Okamura, M. Y.; Fredkin, D. R.; Isaacson, R. A.; Feher, G. In *Tunneling in Biological Systems*; Chance, B., Marcus, R. A., DeVault, D. C., Schrieffer, J. R., Fraunfelder, H., Sutin, N., Eds.; Academic Press: New York, 1979; pp 729−743.